MANAS Journal of Engineering
ISSN 1694-7398 | e-ISSN 1694-7398

Volume 10, Issue 1, (2022) Pages – 1-16
https://doi.org/10.51354/mjen 914000

Performance analysis of static var compensators for distance protection of Nigerian 132-kV sub-transmission network using Matlab/ Simulink model

Akintunde S. Alayande[1], Sunday O. Akınbode[2], Ignatius K. Okakwu[3], Ajibola O. Oyedejı[4,*]

[1] Department of Electrical and Electronics Engineering, University of Lagos, Akoka, Nigeria.
aalayande@unilag.edu.ng
[2] Department of Electrical and Electronics Engineering, University of Lagos, Akoka, Nigeria.
[3] Department of Electrical and Electronics Engineering, Olabisi Onabanjo University, Ago-Iwoye, Nigeria.
okakwu.ignatius@oouagoiwoye.edu.ng
[4] Department of Computer Engineering, Olabisi Onabanjo University, Ago-Iwoye, Nigeria.
oyedeji.ajibola@oouagoiwoye.edu.ng, ORCID: 0000-0002-0180-492X

ABSTRACT

In this paper, the influence of the Static Var Compensators (SVC) on distance relay protection when connected to the sub-transmission network of the Nigerian 132-kV grid system is investigated. This is carried out by monitoring the error margin of the fault locator associated with the distance protective relays when SVC is connected to the transmission line. The location of the SVC is selected such that there is a common primary source of power to the sub-transmission network (Ikorodu-Sagamu 132-kV transmission line) and the SVC, which is a shunt-connected device located on Ikorodu 132-kV bus. The fault is simulated at 33.6 km and 60.4 km respectively from the Ikorodu 132-kV sub-station in MATLAB/ Simulink model and the simulation results obtained are used to investigate the influence of SVC on distance protective relay when connected to the 132-kV power transmission line. The results of the line faults are obtained with respect to earth for both zones one (1) and two (2) when SVC is connected and disconnected for all shunt type of faults. Thus, indicating under-reach and over-reach characteristics of the distance relay, when the SVC is connected and disconnected, while the transmission line protection showed no under-reach or over-reach characteristics for line-to-line fault for both zones with the SVC connected or disconnected. The results of this study show that though SVCs improve the quality of power to consumers, there is a tendency for under-reach and over-reach characteristics of the protective relay to be displayed when the relays are disconnected and connected, which introduces error margins to the fault locator in distance protective relays. Therefore, more detailed dynamic simulations are recommended for reducing the error margin.

ARTICLE INFO

Research article

Received: 12.04.2021
Accepted: 7.02.2022

Keywords:
Static var compensators,
distance relay protection,
error margins,
flexible alternating current transmission systems,
voltage profile

**Corresponding author*

1 Introduction

Static Var Compensators (SVC) are one of the most basic Flexible Alternating Current Transmission Systems (FACTS) available today [2]. SVC's are versatile in their application as they are used to correct and maintain the voltage profiles of power transmission lines and also to improve the amount of power delivered through the transmission lines [2]. The control of reactive power is the SVC's primary responsibility as it either injects or absorbs reactive power when connected to the grid network. When the voltage profile is low, the thyristors trigger the capacitive mode to add reactive power for the voltage profile to return to normal. Similarly, when the voltage profile of the transmission line is high, the thyristors trigger the inductive mode and the SVC adds reactive power for the voltage profile to return to normal [2].

Globally, many industries have employed the use of SVCs due to their dual functionality of maintaining a normal voltage when the network variables or reactive component in the power system are either highly capacitive or inductive [1]. Industries such as power companies, railway, oil & gas companies, steel companies, mining industries have all switched to the use of SVC's because of lower maintenance costs, increased plant and energy efficiency, lower overall

system losses [1]. In Africa, the use of SVC is gaining popularity as companies such as Eskom located in South Africa improved the quality of power delivered by connecting five (5) -50/250MVAR and -10/35MVAR to their 400kV and 132kV power grid respectively [2]. In Nigeria, the popularity of SVC is just getting a boost as the Transmission Company of Nigeria (TCN) is geared towards improving the quality of power delivered. TCN recently commissioned 25-MVar and 60-MVar Fixed Capacitor Banks at Keffi and Apo 132/33kV Substation located at Nassarawa and Abuja (F.C.T.) respectively. The project is an emergency approach aimed at improving the voltage profile being supplied by TCN under the $13 Million Japanese International Cooperation Agency (JICA) grant. NISSIN Electric, a Japanese power company conducted detailed research on the voltage deficit to Abuja and environs [3].

FACTS controllers are numerous and their point of application for optimum performance differ. They are used in distribution and transmission networks for voltage profile correction and reactive power control. Distance protective relays are vital at ensuring distribution and transmission lines are adequately protected in the event of a fault. Electrical signal quantities (Voltage and current) are utilised by the distance protective relay to calculate apparent impedance. The distance protective relay has many types of architectures such as lens, mho, modified, mho, peanut, impedance, quadrilateral and elliptical [4].

This study attempts to focus on the mho architecture for distance protective relays as it can accommodate up to six (6) zones of protection but primarily only four (4) will be considered. These four zones are zone one (1), zone two (2), zone three (3) and zone four (4) which is also known as zone three (3) reverse. Zone one (1) usually covers 80-90% of the protected line, zone two (2) covers 100% of the protected line plus 20-50% of the next neighbouring line, zone three (3) covers 100% of the protected line plus 125% of the next neighbouring line, zone four (4) is a zone with its direction of protection placed in the reverse approach and its reach is 10-25% of the protected line. time and current grading coordination of all protective relays in the grid network must be done to avoid unnecessary tripping [5].

The benefits that could be derived from the application of distance relay protection in power systems are numerous. These include, but not limited to, improving the stability of the grid, providing protection to the transmission network against transient, semi-transient and permanent faults, providing backup protection to the feeder and transformer, increasing the efficiency of the grid network, causing a significant reduction in the maintenance costs and reducing transmission line losses. Besides, the introduction of SVCs as indicated in this research will help at improving grid stability, reduced fluctuations of Voltage profile, reduction in transmission line losses and an improvement in overall grid efficiency. The under-reach and overreach tendencies of distance protective relays for shunt faults observed in this research is a result of the introduction of SVCs.

2. Material and methods

It is well-known that distribution systems are affected by stochastic events such as faults on lines, sudden failures of power plants and random variations in demand.

The occurrence of faults on transmission lines is inevitable. However, the influence of their occurrence is not expected to have a significant impact on the operation of the system by the timely isolation of affected parts from the healthy parts of the system. These faults are usually classified into Line-to-Earth (L-E) fault, Line-to-Line-to-Earth (L-L-E) fault, Line-to-Line-to-Line-to-Earth (L-L-L-E) fault, Line to Line (L-L) fault.

2.1. Single line-to-earth

This is the most common type of fault. It is averaged that 80% of most transmission line faults are single phase to earth in nature. The type of faults can be either a result of lightning strikes, external or internal events. For reference, we will adopt Phase A as our reference phase [6]. If phase A is subjected to SLG fault, as shown in Figure 1, the magnitude of the current flowing through the ground can be expressed as follows:

$$I_{FA} = \frac{V_{AF}}{Z_F} \quad (1)$$

$$I_{FB} = 0 \quad (2)$$

The equivalent circuit is drawn from all the Thevenin's equivalent impedances derived from the zero, negative and positive sequences as shown in Figure 2 [1,6].

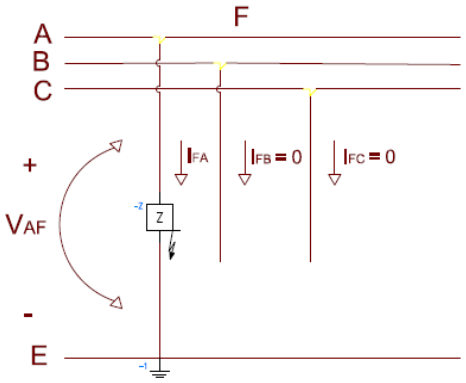

Figure 1. *Diagram showing a Single Line-to-Earth Fault (L-E)* [8].

From equivalent circuit, shown in Figure 2, we can write

$$\begin{bmatrix} I_a \\ I_b \\ I_c \end{bmatrix} = \begin{bmatrix} 1 & 1 & 1 \\ 1 & a^2 & a \\ 1 & a & a^2 \end{bmatrix} \begin{bmatrix} I_{a0} \\ I_{a1} \\ I_{a2} \end{bmatrix} \quad (3)$$

$$I_{a0} = I_{a1} = I_{a2} = \frac{1}{3}(I_a) \quad (4)$$

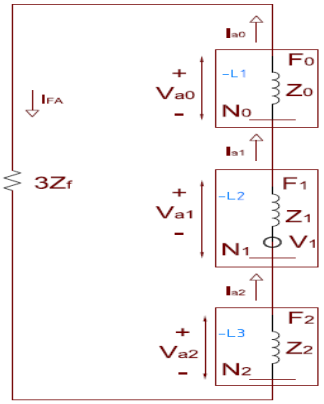

Figure 2. *Sequence diagram for a Single Line-to-Earth Fault (L-E)* [8].

Considering the voltages, we have

$$\begin{bmatrix} V_{a0} \\ V_{a1} \\ V_{a2} \end{bmatrix} = \begin{bmatrix} 0 \\ V_F \\ 0 \end{bmatrix} - \begin{bmatrix} Z_0 + Z_F & 0 & 0 \\ 0 & Z_1 + Z_F & 0 \\ 0 & 0 & Z_2 + Z_F \end{bmatrix} . \begin{bmatrix} I_{a0} \\ I_{a1} \\ I_{a2} \end{bmatrix} \quad (5)$$

Therefore, the fault current through A is

$$I_{FA} = \frac{3\ X\ V_F}{Z_0 + Z_1 + Z_2 + 3Z_F} \quad (6)$$

2.2. Double Line to Earth Fault

This type of fault can easily manifest to L-L-L-E fault if not cleared within the shortest possible time and it is represented in Figure 3. The interconnection of the positive, negative and zero sequence networks is shown in Figure 4.

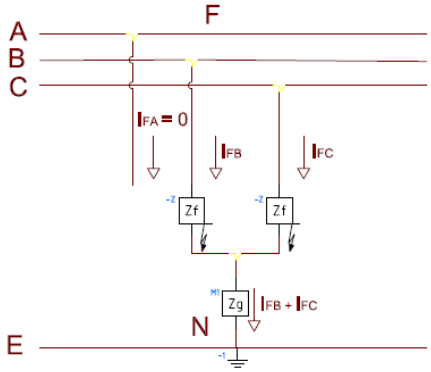

Figure 3. *A Diagram showing a Line-to-line-to-Earth fault (L-L-E)*[8].

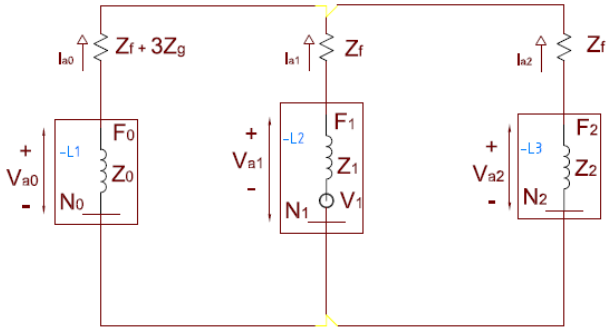

Figure 4. *Sequence for a Line-to-line-to-Earth fault (L-L-E)* [8].

From Figure 4,

$$I_{a1} = \frac{V_F}{(Z_1 + Z_F) + \left(\frac{(Z_2 + Z_F)(Z_0 + Z_F + 3Z_g)}{Z_0 + Z_2 + 2Z_F + 3Z_g}\right)} \quad (7)$$

$$I_{a2} = -\left(\frac{(Z_0 + Z_F + 3Z_g)}{(Z_2 + Z_F)(Z_0 + Z_F + 3Z_g)}\right).I_{a1} \quad (8)$$

$$I_{a0} = -\left(\frac{(Z_2 + Z_F)}{(Z_2 + Z_F)(Z_0 + Z_F + 3Z_g)}\right).I_{a1} \quad (9)$$

If $Z_g = 0$,

$$I_{a1} = \frac{V_F}{(Z_1) + \left(\frac{(Z_2)(Z_0 + 3Z_F)}{Z_0 + Z_2 + 3Z_F}\right)} \quad (10)$$

$$I_{a2} = -\left(\frac{(Z_0 + 3Z_F)}{(Z_2 + Z_0 + 3Z_F)}\right).I_{a1} \quad (11)$$

$$I_{a0} = -\left(\frac{Z_2}{(Z_2 + Z_0 + 3Z_F)}\right).I_{a1} \quad (12)$$

If $Z_F = 0$ & $Z_g = 0$,

$$I_{a1} = \frac{V_F}{(Z_1) + \left(\frac{Z_2 x\ Z_0}{Z_0 + Z_2}\right)} \quad (13)$$

$$I_{a2} = -\left(\frac{Z_0}{(Z_2 + Z_0)}\right).I_{a1} \quad (14)$$

$$I_{a0} = -\left(\frac{Z_2}{Z_2 + Z_0}\right).I_{a1} \quad (15)$$

The total fault current through the neutral is given by

$$I_n = 3I_{a0} = I_B + I_C \quad (16)$$

Considering the voltage equations, we have

$$= \begin{bmatrix} 0 \\ V_F \\ 0 \end{bmatrix} - \begin{bmatrix} Z_0 + Z_F & 0 & 0 \\ 0 & Z_1 + Z_F & 0 \\ 0 & 0 & Z_2 + Z_F \end{bmatrix} . \begin{bmatrix} V_{a0} \\ V_{a1} \\ V_{a2} \end{bmatrix} \begin{bmatrix} I_{a0} \\ I_{a1} \\ I_{a2} \end{bmatrix} \quad (17)$$

For $Z_F = 0 \ and \ Z_g = 0$

$$V_{a0} = V_{a1} = V_{a2} = V_F - (I_{a1}.Z_1) \quad (18)$$

Considering the phase voltages, we have

$$V_A = V_{a0} + V_{a1} + V_{a2} = 3V_{a1} \quad (19)$$
$$V_A = V_C = 0 \quad (20)$$

Considering the line-to-line voltages, we have

$$V_{AB} = V_A - V_B = V_A \quad (21)$$
$$V_{BC} = V_B - V_C = 0 \quad (22)$$
$$V_{CA} = V_C - V_A = -V_A \quad (23)$$

2.3. Three Phase-to-Earth Fault

A balanced three-phase fault is shown in Figure 5 whose impedance diagram is depicted in Figure 6. It is the most severe type of fault but rarely occurs. The zero and negative sequences are zero in this type of fault. Consequently, only the positive sequence represents the interpretation of the fault. When the magnitude of the fault voltage is not known, it is usually assumed to be 1.05∠0°V [7].

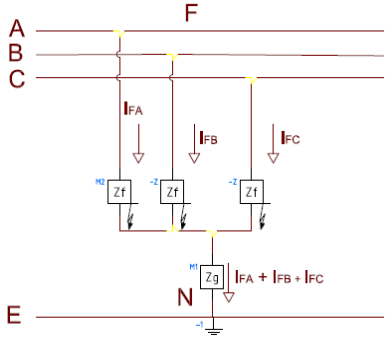

Figure 5. *A Line-to-Line-to-Line-to-Earth fault (L-L-L-E)* [8].

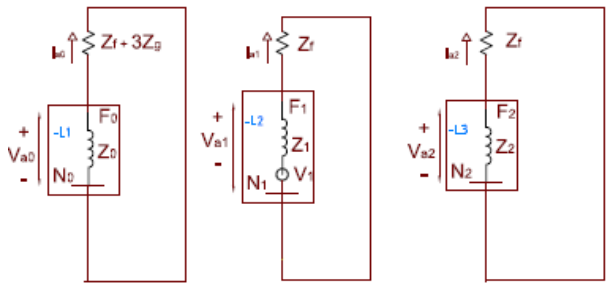

Figure 6. *Sequence network for a Line-to-Line-to-Line-to-Earth fault (L-L-L-E)* [8].

From Figure 6, the phase voltages are,

$$V_A = I_A Z_F = V_{a1} \quad (24)$$
$$V_B = a^2 V_{a1} \quad (25)$$
$$V_C = aV_{a1} \quad (26)$$

The line-to-line voltages can be expressed as

$$V_{AB} = V_A - V_B = (1 - a^2)V_A = \sqrt{3} I_a Z_F \angle 30° \quad (27)$$
$$V_{BC} = V_B - V_C = (a^2 - a)V_A = \sqrt{3} I_a Z_F \angle -9 \quad (28)$$
$$V_{CA} = V_C - V_A = (a - 1)V_A = \sqrt{3} I_a Z_F \angle 150° \quad (29)$$

2.4. Phase-to-Phase Fault

This is a fault that occurs on the two phases B and C simultaneously as shown in Figure 7. The sequence network for such a system is shown in Figure 8 and the resulting equations are as follows:

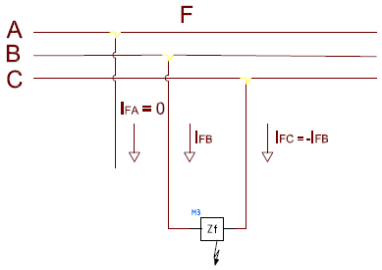

Figure 7. *A diagram showing a Line-Line fault (L-L)* [8].

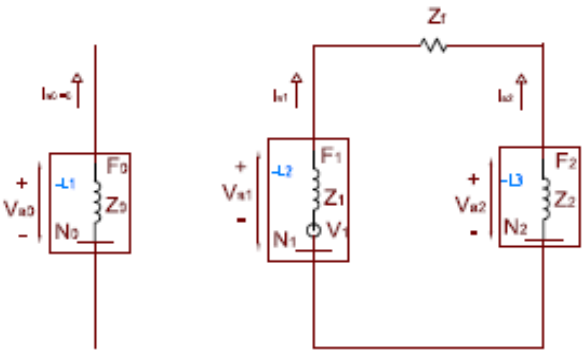

Figure 18. *Network sequence for a Line-Line fault (L-L)* [8]

$$I_A = 0 \quad (30)$$
$$I_B = -I_C \quad (31)$$
$$I_{a1} = -I_{a2} \quad (32)$$
$$V_B - V_C = I_B Z_F \quad (33)$$
$$\begin{bmatrix} I_{a0} \\ I_{a1} \\ I_{a2} \end{bmatrix} = \frac{1}{3} . \begin{bmatrix} 1 & 1 & 1 \\ 1 & a & a^2 \\ 1 & a^2 & a \end{bmatrix} . \begin{bmatrix} 0 \\ I_B \\ -I_B \end{bmatrix} = \begin{bmatrix} 0 \\ (a - a^2)I_B \\ (a^2 - a)I_B \end{bmatrix} \quad (34)$$

When

$$V_{a0} = 0, I_{a1} = -I_{a2} = \frac{V_F}{Z_1 + Z_2 + Z_F} \quad (35)$$

The current through the phase B and the phase voltages at A, B and C are expressed respectively as

$$I_B = \frac{j\sqrt{3}V_F}{Z_1 + Z_2 + Z_F} = \frac{\sqrt{3}\angle 90°X\ V_F}{Z_1 + Z_2 + Z_F} \quad (36)$$

$$\begin{bmatrix} V_A \\ V_B \\ V_C \end{bmatrix} = \begin{bmatrix} 1 & 1 & 1 \\ 1 & a^2 & a \\ 1 & a & a^2 \end{bmatrix} \begin{bmatrix} 0 \\ V_{a1} \\ V_{a2} \end{bmatrix} \quad (37)$$

The line-to-line voltages are then

$$V_{AB} = V_A - V_B \quad (38)$$
$$V_{BC} = V_B - V_C \quad (39)$$
$$V_{CA} = V_C - V_A \quad (40)$$

2.5. Concept of distance protection

To accurately determine the fault point on a very long transmission line, a distance relay is of utmost importance. Consider the circuit shown in Figure 9, it is assumed that the relay is located at point A and the relay has a reach of Zset. If an internal fault occurs (F1), the relay will trip but if an external fault occurs (F3) the relay will be restrained. From Figure 9, Distance relay zones can be mainly categorised into three (3) zones of protection. Zone 1, Zone 2 and Zone 3.

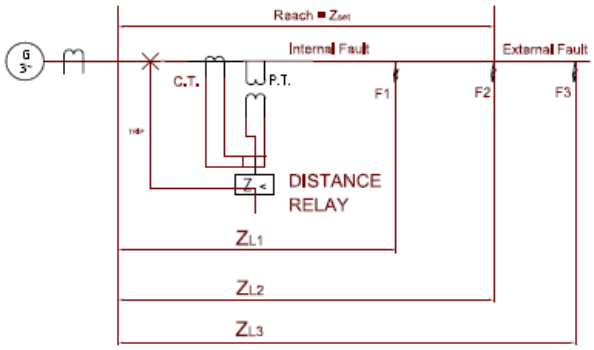

Figure 9. *Zones of protection of a transmission line*

2.6. Choice between Impedance, Reactance and Mho Algorithm

The reactance relay is preferred for use as a grounding relay because it is more stable when used on short lines rather than long lines. Consequently, the relay becomes unstable during power surges unless if an additional relay is installed to prevent such mal-operation. Mho type is preferred for phase-to-phase faults, long line and lines with heavy power surges. When a mho relay is used for the protection of a line section, its operating characteristics cover the least space in the R-X diagram. Impedance relay is preferred for phase faults related to lines of moderate length. Arc resistance affects impedance relay more than reactance relay but less than mho distance relay. In this paper, mho relay is explored for our analysis [9].

3. Results and discussions

The one-line diagram of the network used as a case study is as shown below;

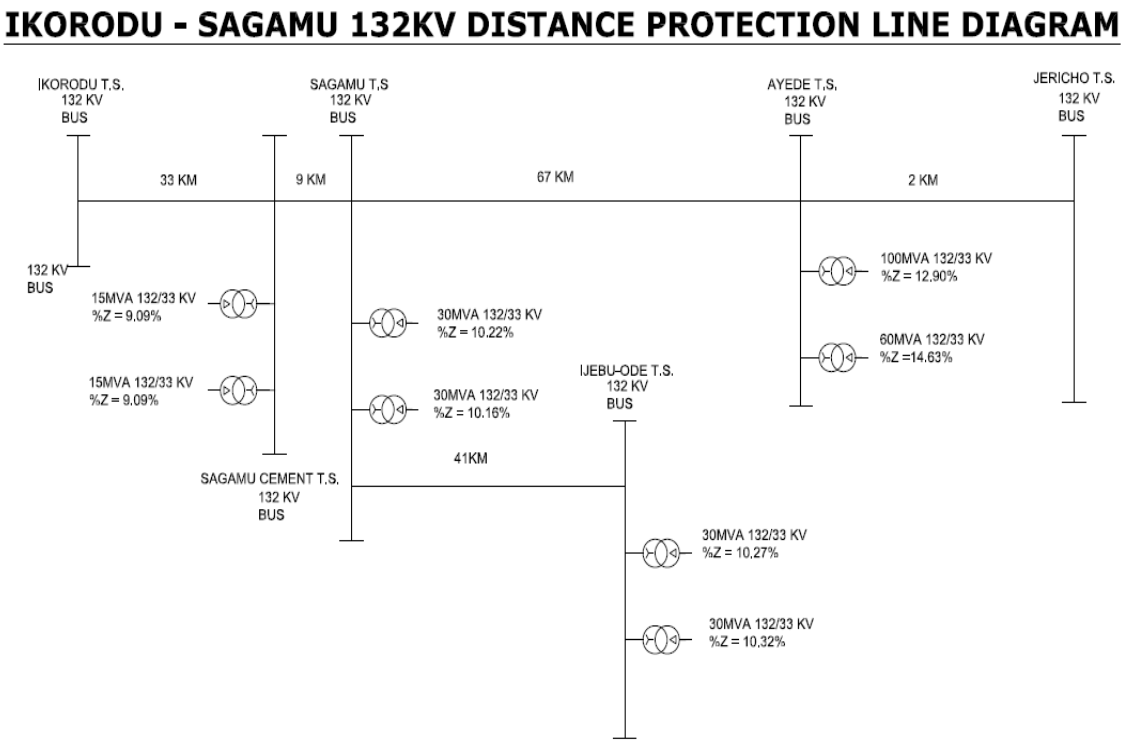

Figure 10. *One line diagram of Ikorodu-Sagamu 132kV distance protective scheme*

A brief description of each of the components modelled in the MATLAB/ SIMULINK environment is presented as follows:

3.1. The Distance Relay Simulink Model

The MATLAB/SIMULINK simulation is used to model a variety of protective relays through current measurement (which represents the current transformer), voltage measurement (which represents the voltage transformer), logic operations, Math operators, signal attributes and routing etc.

The distance relay is accurately modelled through the measurement of current and voltage parameters. The measured impedance is compared to the calculated impedance setting of the line, thus, the zone in which the fault impedance occurs is identified. The distance relay also sends out a trip signal to the circuit breaker to isolate the faulted area of the network [6]. In MATHLAB/SIMULINK, each block is separately modelled and thereafter connected. The main blocks responsible for the proper modelling and operation of the distance relay, in this paper, include Fault Detection & Identification Block, Impedance Measurement Block, Zone Detection & Time delay Block, Fault Locator Block and Tripping Signal Block [6]. The complete model for the transmission line incorporated with a distance relay and the SVC is depicted in Figure 10. The Static Var compensator (SVC) is a shunt connected device and it is usually applied at the primary location of the distance relay. In this study, our primary location is Ikorodu 132/33kV Sub-Station. In our study, we considered an SVC designed by Pierre Giroux and Gibert Sybille (Hydro-Quebec) for (MATHWORKS) MATLAB which is sized as one (1) no Thyristor controlled reactor (TCR) 109MVAR and three (3) nos Thyristor switched Capacitor (TSC) of 94MVAR each. The +300MVar/-100MVar SVC model designed by Pierre Giroux and Gibert Sybille (Hydro-Quebec) is connected to a 735kV 60Hz transmission line and 200MW load. The SVC model Voltage and frequency parameters were adjusted to match our input voltage of 132kV and 50Hz respectively while all other parameters remained the same as the original model designed [10].

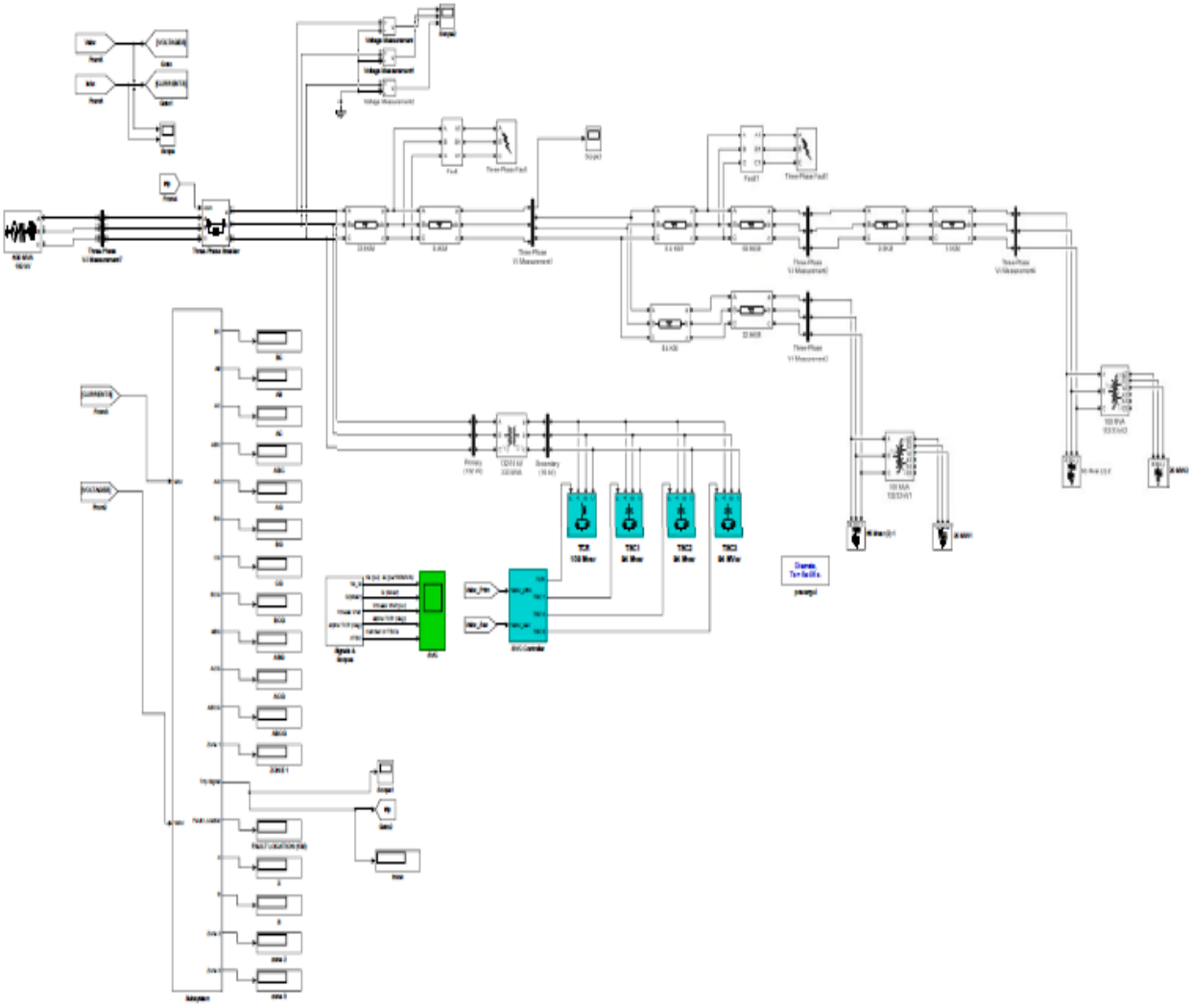

Figure 11. *The Complete transmission line, distance relay and static var compensator model.*

3.2. The mho circle characteristics simulink model

The Mho Characteristic graph is drawn using the MATLAB M-file and it shows the relationship between resistance and reactance on a transmission line. In Figure 12, each Mho circle represents a zone of protection as illustrated by the Legend of the Mho Circle Graph. MATLAB codes was used for representing the zones of protection on a Mho Circle Graph. Figure 12 shows the picture of the Mho Circle Characteristics graph.

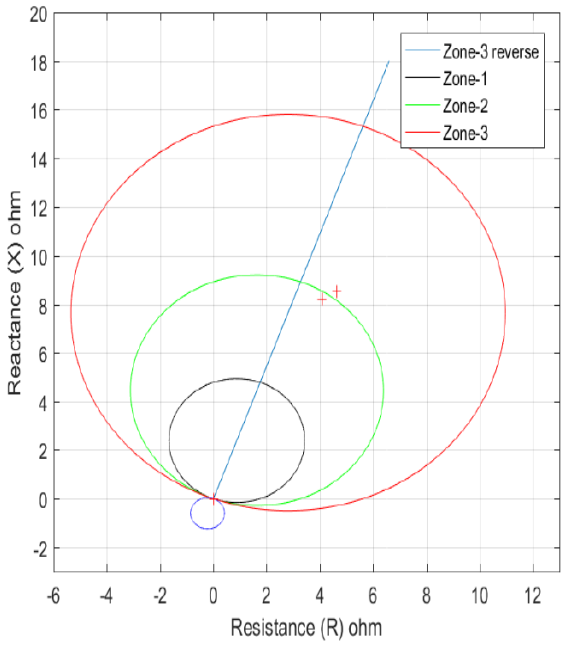

Figure 12. *Mho Circle plot*

3.3.The Complete Distance Relay Simulink Model

The complete distance relay as shown in Figure 13 is a combination of the fault detection and identification block, impedance measurement block, zone detection and time delay block, fault locator block and the mho circle characteristics graph.

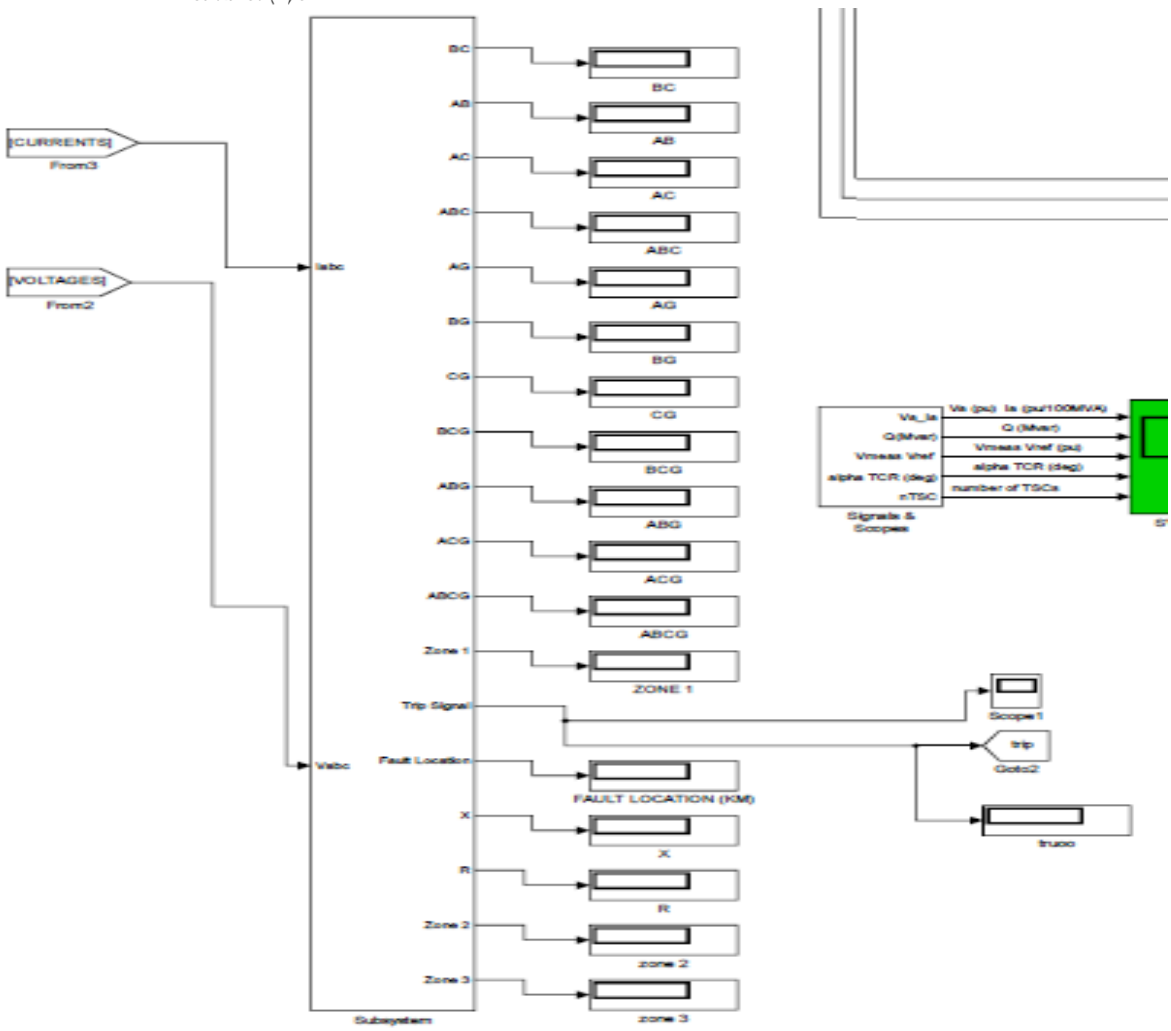

Figure 13. *The Complete Distance Relay Model*

3.4.The Static Var Compensator (Svc) Simulink Model

SVCs are shunt-connected devices. This particular model of SVC was designed by Pierre Giroux and Gibert Sybille (Hydro-Quebec) for (MATHWORKS) MATLAB and used to study the impact of harmonics, transients and stresses on power components during fault conditions. The model has been modified to fit the parameters of this research project which seeks to understand the consequence of SVC on transmission line protection.

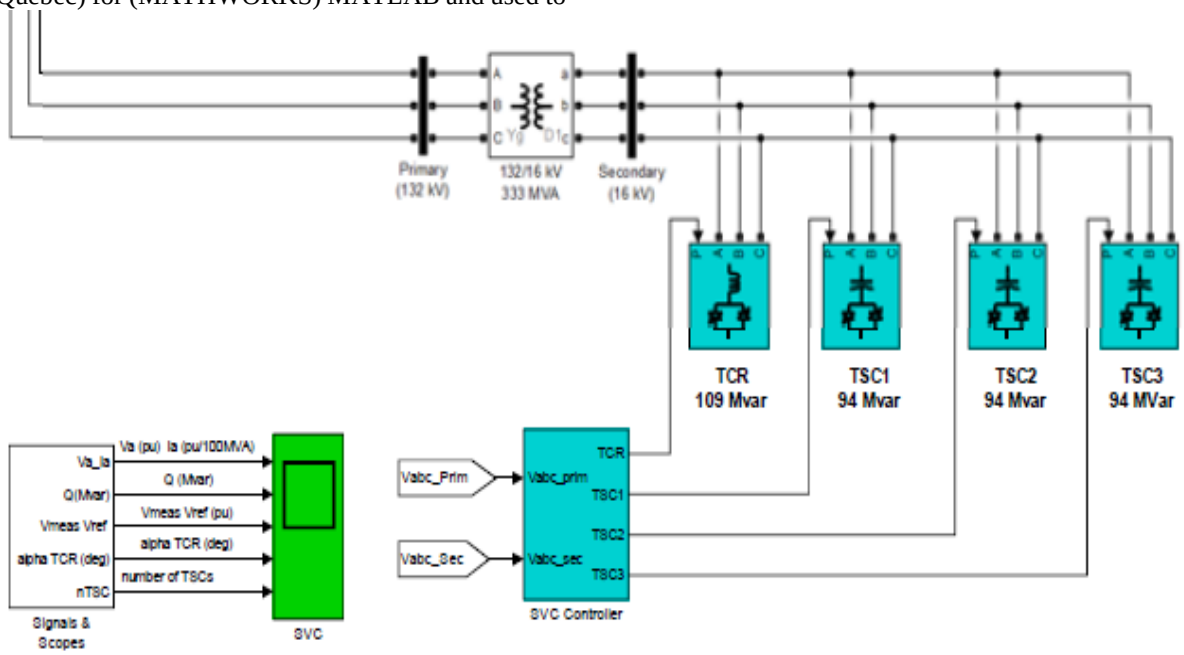

Figure 14. *The Static Var Compensator (SVC) model*

The SVC model has one (1) TCR of 109MVAR rating, three (3) TSC of 94MVAR rating each and an SVC Controller [10]. The modifications that affected this model includes modifying the voltage and frequency parameters to suit the required parameters for this paper. Figure 14 shows the basic structure of the SVC model used for the simulation.

3.5.The Svc Control System

The SVC control system is responsible for the controlled firing of the thyristors to inject or absorb VAR into the system based on the inherent system parameters. The SVC Control system consists of four (4) components which include the measurement system, voltage regulator, distribution unit and firing unit [9,11].

The simulations were carried out considering faults occurring in zone one (1) and zone two (2) of the distance relay protective scheme. The results obtained are presented in Table 1.

Table 1. *Simulation result for the impedance and fault location as seen by the distance relay modelled in MATLAB/Simulink*

Protection zone	SVC connection status		Types of fault				
			L-E fault	L-L fault	L-L-L fault	L-L-E fault	L-L-L-E fault
zone 1	with svc	apparent impedance	2.296 + j4.553 (5.099)	1.698 + j3.752 (4.118)	1.997 + j4.954 (5.341)	2.296 + j4.551 (5.097)	1.997 + j4.153 (4.608)
		fault location	33.6 km	27.14 km	35.19 km	33.58 km	30.36 km
zone 1	without svc	apparent impedance	2.296 + j4.553 (5.099)	1.698 + j3.752 (4.118)	1.997 + j4.954 (5.341)	1.824 + j3.888 (4.295)	1.997 + j4.954 (5.341)
		fault location	33.6 km	27.14 km	35.19 km	28.29 km	35.19 km
summary for zone 1 distance relay			Same	Same	Same	over reach	under reach
zone 2	with svc	apparent impedance	4.073 + j8.211 (9.166)	4.066 + j8.201 (9.154)	4.066 + j8.777 (9.672)	4.073 + j8.211 (9.166)	4.073 + j8.211 (9.166)
		fault location	60.39 km	60.31 km	63.73 km	60.39 km	60.39 km
zone 2	without svc	apparent impedance	4.073 + j8.766 (9.666)	4.066 + j8.202 (9.155)	4.066 + j8.776 (9.672)	4.073 + j8.766 (9.666)	4.073 + j8.767 (9.666)
		fault location	63.69 km	60.32 km	63.73 km	63.69 km	63.69 km
summary for zone 2 distance relay			under reach	Same	Same	under reach	under reach

Table 1 presents the results obtained when the SVC is connected and disconnected from the transmission line for both faults in zone 1 and zone 2. As shown in Table 1, our analysis was based on the simulation of five different types of faults on the network considering zone one (1) and zone two (2). For instance, in zone one (1), considering the Single Line-to-Earth (L-E) fault, the Resistance-Reactance (R-X) diagram for the distance relay when SVC is connected with the transmission line is shown in Figure 15 (a) while Figure 15 (b) shows the Resistance-Reactance (R-X) diagram for the distance relay when SVC is not connected for the same L-E type of fault. Figure 15a and Figure 15b clearly show plotted points (purple and red) at the same magnitude of Resistance (R) of 2.296Ω and Reactance (X) j4.553Ω as shown in Table 1 for both Line-to-Earth faults with and without the SVC connected to the bus. Consequently, in both conditions, the distance relay was observed to have tripped at 33.6km. Thus, indicating that during line-to-earth (L-E) fault conditions with SVC connected or not connected the distance relay fault location accuracy is not affected.

When the simulation is carried out for Phase-to-Phase (L-L) faults, the Resistance-Reactance (R-X) diagram for the distance relay when SVC is connected with the transmission line is shown in Figure 16 (a) while the Resistance-Reactance (R-X) diagram for the same Phase-to-Phase (L-L) fault with the distance relay but without the SVC is shown in Figure 16 (b). Figure 16a and Figure 16b clearly show plotted points (purple and red) at the same magnitude of Resistance (R) of 1.698Ω and Reactance (X) j3.752Ω as shown in Table 1 for both Line-to-Earth faults with and without the SVC connected to the bus. Consequently, in both conditions, the distance relay was observed to have tripped at 27.14km. Thus, indicating that during Phase-to-Phase (L-L) fault conditions with SVC connected or not connected, the distance relay fault location accuracy is not affected.

For Double-Line-to-Earth faults (L-L-E), Figure 17 (a) shows the Resistance-Reactance (R-X) diagram for the distance relay when SVC is connected while Figure 17 (b) shows the Resistance-Reactance (R-X) diagram for the distance relay when SVC is not connected. Figure 17a and Figure 17b clearly show plotted points (purple and red) at the different magnitude of Resistance (R) and Reactance (X). The purple plotted dot in Figure 17 (a) has a Resistance (R) magnitude of 2.296Ω and Reactance (X) Magnitude of j4.551Ω as shown in Table 1 for Double-Line-to-Earth (L-L-E) with SVC connected while the red plotted dot in Figure 17 (b) has a Resistance (R) magnitude

of 1.824Ω and Reactance (X) Magnitude of j3.888Ω as shown in Table 1 for Double-Line-to-Earth (L-L-E) without SVC connected. Consequently, the distance relay, with and without SVC connected was observed to have tripped at 33.58km and 28.29km respectively. Thus, indicating that during Double-line-to-Earth (L-L-E) fault conditions, the distance relay over-reaches with the SVC connected.

For Three-Phase-to-Earth faults (L-L-L-E), Figure 18 (a) shows the Resistance-Reactance (R-X) diagram for the distance relay when SVC is connected while Figure 18 (b) shows the Resistance-Reactance (R-X) diagram for the distance relay when SVC is not connected. Figure 18a and Figure 18b clearly show plotted points (purple and red) at the same magnitude of Resistance (R) and different magnitude of Reactance (X). The purple plotted dot in Figure 18 (a) has a Resistance (R) magnitude of 1.997Ω and Reactance (X) Magnitude of j4.153Ω as shown in Table 1 for Three-phase-to-Earth (L-L-L-E) with SVC connected while the red plotted dot in Figure 18 (b) has a Resistance (R) magnitude of 1.997Ω and Reactance (X) Magnitude of j4.954Ω as shown in Table 1 for Three-phase-to-Earth (L-L-L-E) without SVC connected. Consequently, the distance relay, with and without SVC connected was observed to have tripped at 30.36km and 35.19km respectively. Thus, indicating that during Three-phase-to-Earth (L-L-L-E) fault conditions, the distance relay under-reaches with the SVC connected.

a

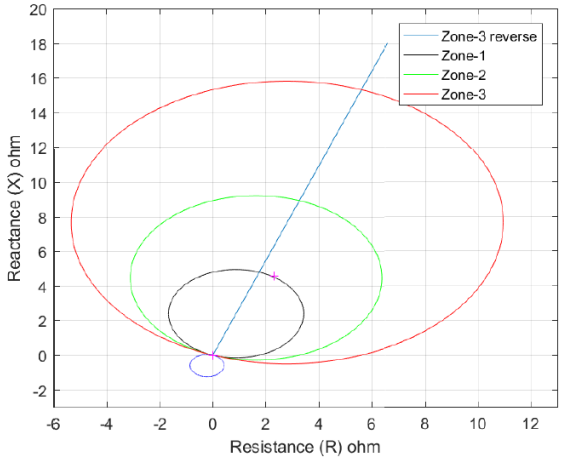

b

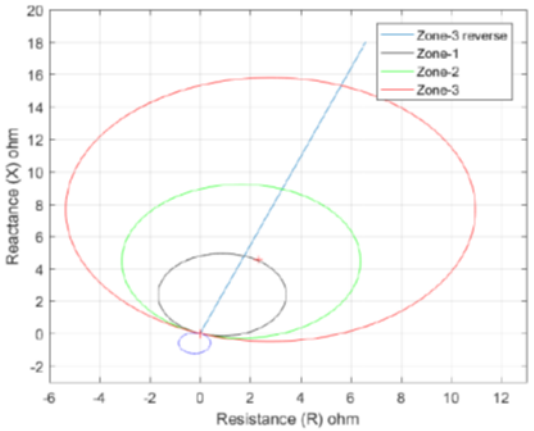

Figure 15. *Resistance-Reactance (R-X) plot of a zone 1 for Line-to-Earth (L-E) fault with (a) with SVC (b) without SVC*

a

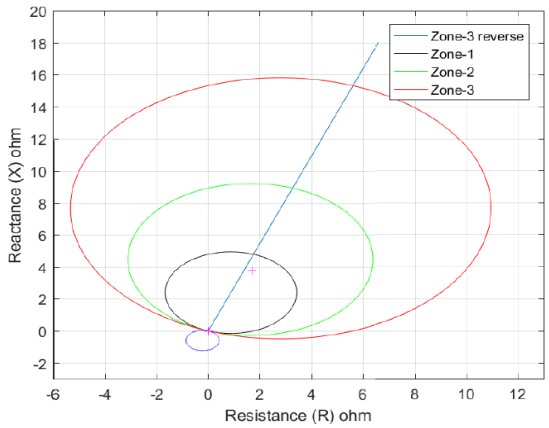

b

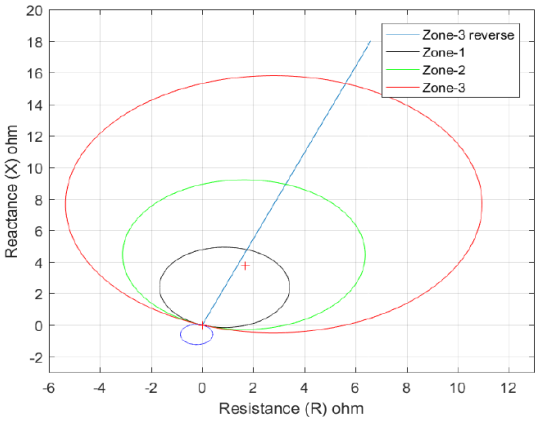

Figure 16. *Resistance-Reactance (R-X) plots of a zone 1 for Phase-to-Phase (L-L) fault with (a) with SVC (b) without SVC*

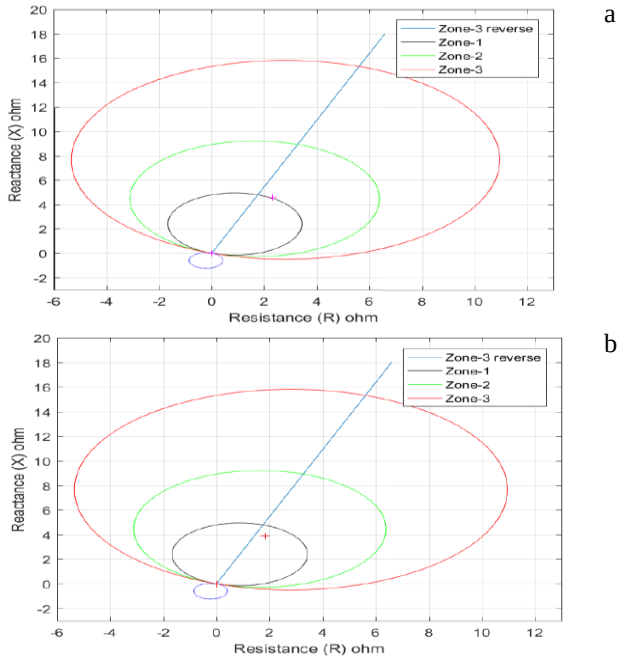

Figure 17. *Resistance-Reactance (R-X) plots of a zone 1 for Double-Line-to-Earth (L-L-E) fault with (a) with SVC (b) without SVC*

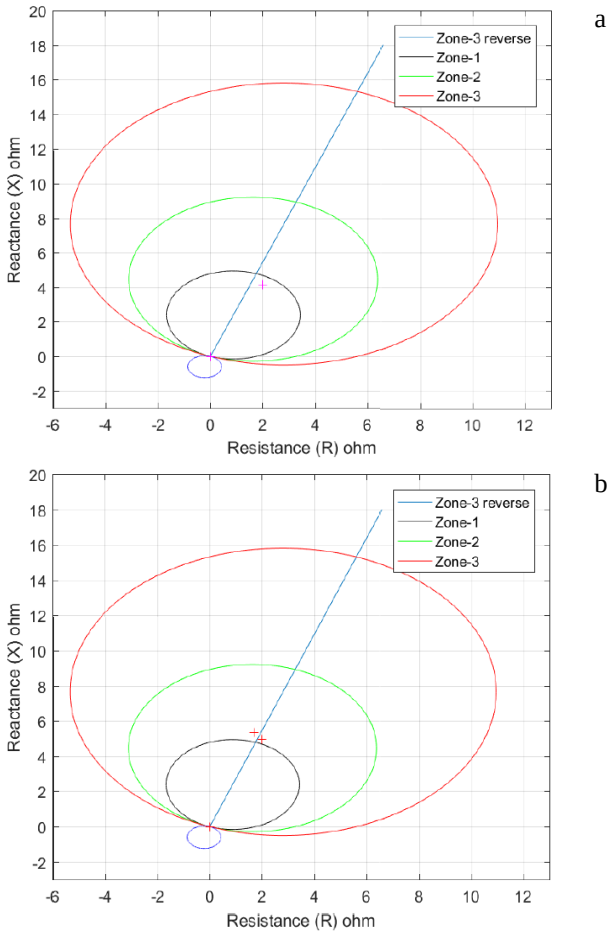

Figure 18. *Resistance-Reactance (R-X) plots of a zone 1 for Three-phase-to-Earth (L-L-L-E) fault with (a) with SVC (b) without SVC*

Considering zone 2, for Single Line-to-Earth (L-E) fault the Resistance-Reactance (R-X) diagram for the distance relay when SVC is connected with the transmission line is shown in Figure 19 (a) while Figure 19 (b) shows the Resistance-Reactance (R-X) diagram for the distance relay when SVC is not connected for the same Single Line-to-Earth (L-E) type of fault. Figure 19a and Figure 19b clearly show plotted points (purple and red) at the same magnitude of Resistance (R) and different magnitude of Reactance (X). The purple plotted dot in Figure 19 (a) has a Resistance (R) magnitude of 4.073Ω and Reactance (X) Magnitude of j8.211Ω as shown in Table 1 for Single Line-to-Earth (L-E) with SVC connected while the red plotted dot in Figure 19 (b) has a Resistance (R) magnitude of 4.073Ω and Reactance (X) Magnitude of j8.766Ω as shown in Table 1 for Single Line-to-Earth (L-E) without SVC connected. Consequently, the distance relay, with and without SVC connected was observed to have tripped at 60.39km and 63.69km respectively. Thus, indicating that during Single Line-to-Earth (L-E) fault conditions, the distance relay under-reaches with the SVC connected.

When the simulation is carried out for the Phase-to-Phase (L-L) faults, the Resistance-Reactance (R-X) diagram with the connection of the distance relay and installation of the SVC is shown in Figure 20 (a) while the Resistance-Reactance (R-X) diagram for the same L-L fault with the distance relay but without the SVC is shown in Figure 20 (b). Figure 20a and Figure 20b clearly show plotted points (purple and red) at the same magnitude of Resistance (R) of 4.066Ω and Reactance (X) j8.201Ω as shown in Table 1 for both Phase-to-Phase (L-L) faults with and without the SVC connected to the bus. Consequently, in both conditions, the distance relay was observed to have tripped at 60.32km. Thus, indicating that during phase-to-phase (L-L) fault conditions with SVC connected or not connected, the distance relay fault location accuracy is not affected.

For Double-Line-to-Earth faults (L-L-E), Figure 21 (a) shows the Resistance-Reactance (R-X) diagram for the distance relay when SVC is connected while Figure 21 (b) shows the Resistance-Reactance (R-X) diagram for the distance relay when SVC is not connected. Figure 21 (a) and Figure 21 (b) clearly shows plotted points (purple and red) at different magnitude of Resistance (R) and Reactance (X). The purple plotted dot in Figure 21 (a) has a Resistance (R) magnitude of 4.073Ω and Reactance (X) Magnitude of j8.766Ω as shown in Table 1 for Double-Line-to-Earth (L-L-E) with SVC connected while the red plotted dot in Figure 21 (b) has a Resistance (R) magnitude of 4.073Ω and Reactance (X) Magnitude of j8.766Ω as shown in Table 1 for Double-Line-to-Earth (L-L-E) without SVC connected. Consequently, the distance relay, with and without SVC connected was observed to have tripped at 60.39km and 63.69km respectively. Thus, indicating that during Double-line-to-Earth (L-L-E) fault

conditions, the distance relay under-reaches with the SVC connected.

For Three-phase-to-Earth faults (L-L-L-E), Figure 21 (a) shows the Resistance-Reactance (R-X) diagram for the distance relay when SVC is connected while Figure 22 (b) shows the Resistance-Reactance (R-X) diagram for the distance relay when SVC is not connected. Figure 22 (a) and Figure 22 (b) clearly shows plotted points (purple and red) at the same magnitude of Resistance (R) and different magnitude of Reactance (X). The purple plotted dot in Figure 22 (a) has a Resistance (R) magnitude of 4.073Ω and Reactance (X) Magnitude of j8.211Ω as shown in Table 1 for Three-phase-to-Earth (L-L-L-E) with SVC connected while the red plotted dot in Figure 22 (b) has a Resistance (R) magnitude of 4.073Ω and Reactance (X) Magnitude of j8.767Ω as shown in Table 1 for Three-phase-to-Earth (L-L-L-E) without SVC connected. Consequently, the distance relay, with and without SVC connected was observed to have tripped at 60.39km and 63.69km respectively. Thus, indicating that during Three-phase-to-Earth (L-L-L-E) fault conditions, the distance relay under-reaches with the SVC connected.

a

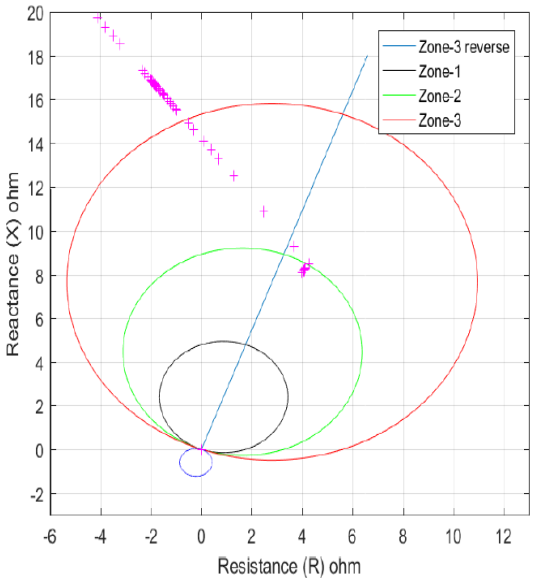

b

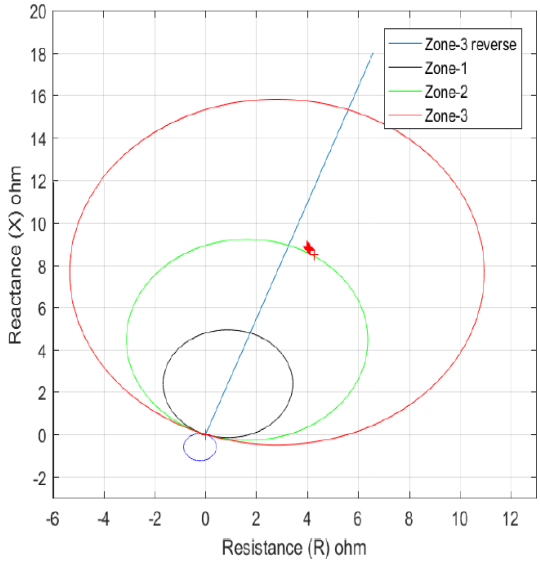

Figure 19. *Resistance-Reactance (R-X) plots of a zone 2 for Single Line-to-Earth (L-E) fault with (a) with SVC (b) without SVC*

a

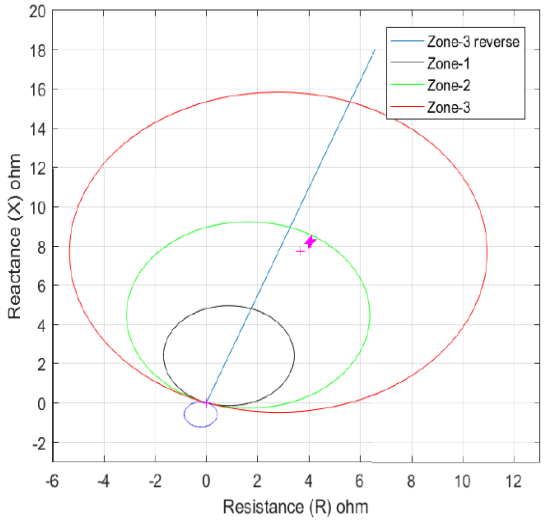

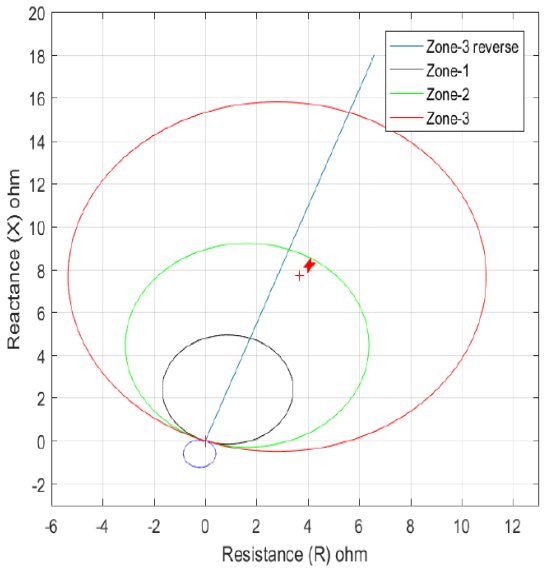

b

Figure 20. *Resistance-Reactance (R-X) plots of a zone 2 for Phase-to-Phase (L-L) fault with (a) with SVC (b) without SVC*

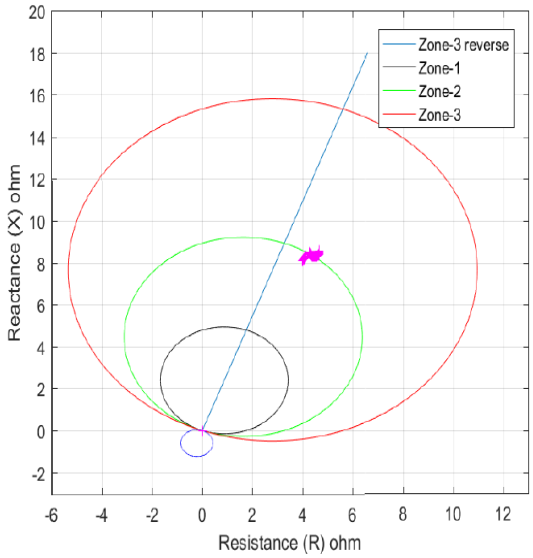

a

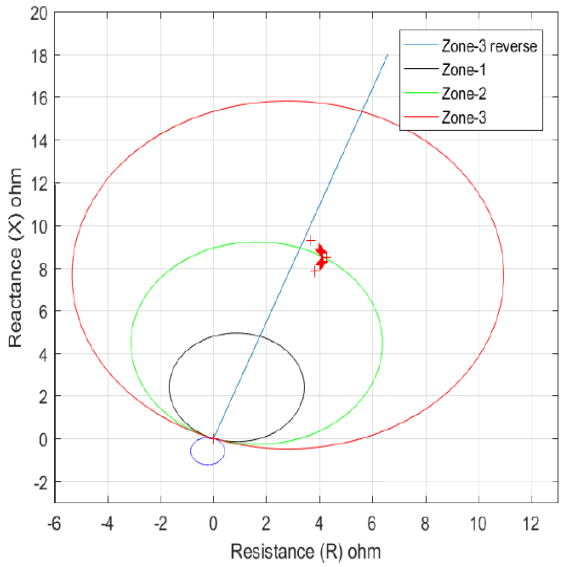

b

Figure 21. *Resistance-Reactance (R-X) plots of a zone 2 for Double-Line-to-Earth (L-L-E) fault with (a) with SVC (b) without SVC*

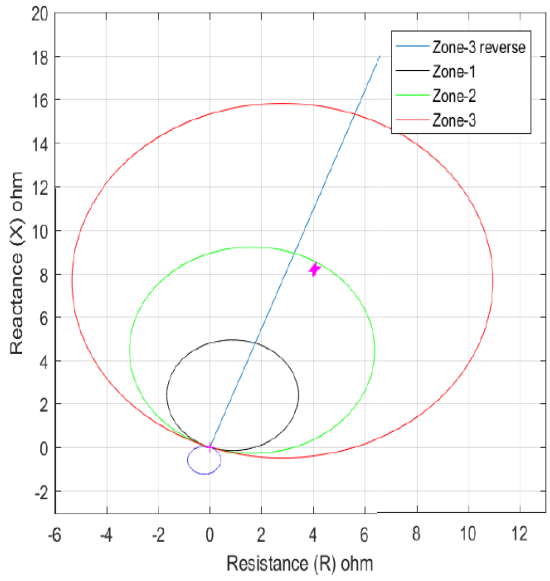

a

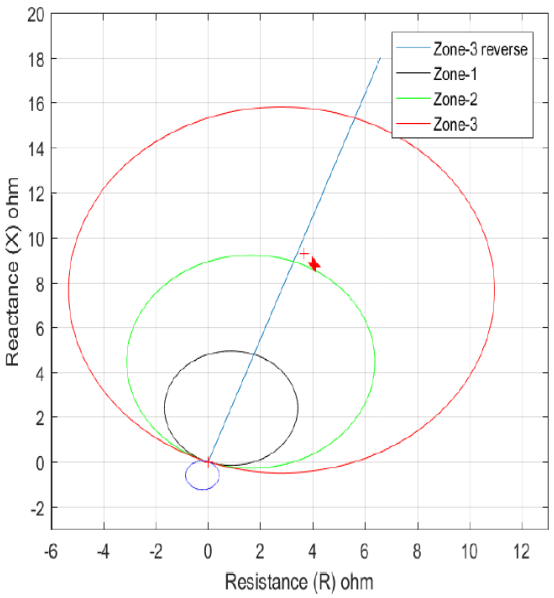

b

Figure 22. *Resistance-Reactance (R-X) plots of a zone 2 for Three-Phase-to-Earth (L-L-L-E) fault with (a) with SVC (b) without SVC*

3.6.Summary of Results

The simulation result when a highly inductive load of 130MVAR is applied into the real-life scenario setting of the Ikorodu-Sagamu 132kV transmission line setting being fed from a source of 600MVA short circuit. The simulation result shows a case of very high voltage despite the highly inductive load due to the surplus amount of source power. From the simulation results obtained for zone one (1) and zone two (2) as represented in Table 1 and Figure 23, the following observations were made during the simulation;

The known fault application points are 33.6km and 60.4km respectively. When SVC is applied, the simulation result shows us that the SVC takes care of the over-voltage condition by stabilizing the voltage, as this is evident in the fault location results, which are close to the applied point of fault. Table 1 shows that the fault locations for both zone one (1) and zone two (2) lies close to the point of fault application. For zone one (1), the fault is applied at 33.6km (80% of protected line settings) and the distance relay sees fault locations such as 33.6km, 27.14km, 35.19km, 33.58km, 30.36km and 28.29km. For zone two (2), the fault is applied at 60.4km (143.8% of protected line settings) and the distance relay sees fault locations such as 60.39km, 60.31km, 63.73km, 63.69km and 60.32km.

Furthermore, the distance protective relays see these fault locations as either over-reach or under-reach. The over-reach and under-reach are evidence that error margins are introduced when SVCs are connected. Static Var Compensators do not affect Phase to phase faults. The tabulated data of Table 1 and plotted dots in Figure 16 and Figure 20 clearly shows that for Phase-to-Phase (L-L) faults, the distance protective relay sees the same magnitude of Resistance (R) and Reactance (X) for both zone one (1) and zone two (2). Similarly, Figure 23 shows a Bar chart comparison for each fault type with and without SVC connected. The similar magnitudes of Resistance (R) and reactance (X) for both zone one (1) and zone two (2) can easily be seen deduced.

Static Var Compensators appear to be more consistent in their operation for zone two (2) faults. From the tabulated data in Table 1, the result shows that for all shunts faults in zone two (2), the distance protective relay under-reaches for all shunt faults to Earth faults and no effect for all phase to phase faults. For zone 1, the distance protective relay under-reaches for Three-Phase-to-Earth (L-L-L-E), over-reaches for Double-Line-to-Earth (L-L-E) and no effect for all phase-to-phase faults (L-L) and Single Line-to-Earth (L-E) faults. Figure 22 shows graphically that zone two (2) fault results appear to be more consistent for all shunt faults, unlike zone one (1) shunt faults which varies from no effect to under-reach and over-reach distance relay tendencies.

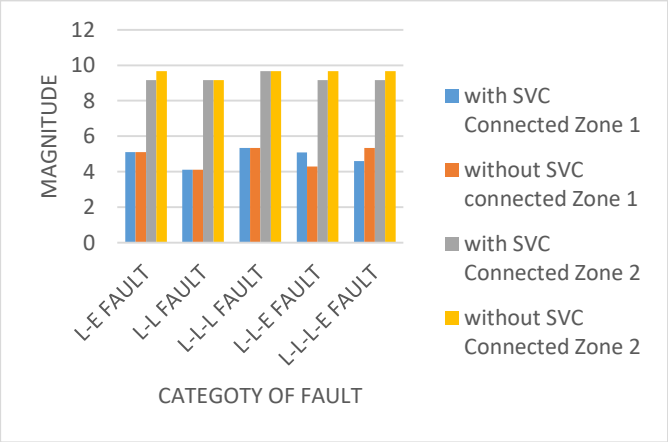

Figure 23. *Distance relay response with and without the installation of SVC*

1. Conclusion

The efficiency of transmission lines is very vital. The need to expand the grid means that the quality of power supplied must be improved upon. The use of Static VAR Compensators is encouraged by its lower cost compared to STATCOM. In this research, the results gotten and analysed satisfies the objectives of this study. The study's comparison of results between when an SVC is connected to the transmission grid and without the SVC connected shows that there are under-reach and over-reach tendencies for faults that occur both in Zone one (1) and Zone two (2).

Figure 22 clearly shows the under reach and overreach fault locations of the distance protective relay when different types of fault occur. The research revealed that for Phase-to-Phase

(L-L) faults in both Zone One (1) and Zone Two (2), they are unaffected by the presence of SVC in the grid network. From Figure 22, the magnitude of Resistance (R) and Reactance (X) for both phase-to-phase (L-L) faults of zone one (1) with and without SVC connected are the same. Similarly, the magnitude of Resistance (R) and Reactance (X) for both Phase-to-Phase (L-L) faults of zone two (2) with and without SVC connected are the same.

It is of paramount importance to note that there is an error margin when an SVC is connected to the transmission grid and without the SVC connected. The under-reach and over-reach tendencies are clear proofs that the relay sees an error margin when the SVC is connected for both zone one (1) and zone two (2). However, the distance protective relays did not show any error margins to Phase-to-Phase (L-L) faults for both scenarios. Site Adaptive setting is encouraged to be implemented since each line section has various parameters introducing errors into the fault location calculations as seen by the distance relays.

Further research on algorithm development to mitigate the inaccuracies in fault locator introduced by the presence of SVC in the Transmission Company of Nigeria (TCN) 132kV Power Grid Network. Further study in the use of other types of FACTS devices is highly recommended using this same methodology. Researchers can also simulate Zone three (3) zone of protection to show if the same behaviours in this research are observed.

Although, the linear predictor is used to obtaining forecast values in this study, it is recommended that other approaches such as Auto-Regressive Moving Average (ARMA) model can be used to enhance the accuracy of the model equation. Also, the study can be further carried out to show the trend of individual fault occurrence which will help the transmission company to have better plans towards mitigation the occurrence of faults and maintenance strategy so as to improve customer satisfaction.

References

[1]. IndustryArc, “Static VAR Compensator Market: By Type (Thyristor-Based SVC, & Magnetically Controlled Reactor-Based SVC) By End-Use Industry (Electric Utility, Renewable, Railway, Industrial, Oil & Gas, & Others), By Component & Geography - Forecast (2018 - 2023),” 2018. [Online]. Available: https://industryarc.com/Report/15449/static-var-compensator-market.html.

[2]. P.S. (AEG G. H. Pesch, S. Ranade, M. Schubert, “Static VAR-Compensators for stabilizing traction and transmission systems in South Africa,” Berlin, 2007.

[3]. Anumihe, “FG obtains $13m JICA grant to fix power supply in Nasarawa State,” Sun News Online, 2019. [Online]. Available: https://www.sunnewsonline.com/fg-obtains-13m-jica-grant-to-fix-power-supply-in-nasarawa-state/. [Accessed: 19-Nov-2020].

[4]. Aptransco, Technical Reference Book. HYDERABAD: TRANSMISSION CORPORATION OFANDHRA PRADESH LIMITED, 2004.

[5]. Mohamed Zellagui A.C., “Impact of svc devices on distance protection setting zones in 400 kv transmission line,” U.P.B. Sci. Bull., Ser. C, (2013), 75, 2, 249–262.

[6]. Lamture J., “DEVELOPMENT OF DISTANCE RELAY IN MATLAB,” Int. J. Adv. Comput. Eng. Netw., (2015), 3, 9, 77–80.

[7]. . Xiaoyao Zhou H.W Aggarwall R.K., Phil Beaumont, “The Impact of STATCOM on Distance Relay,” in 15th Power Systems Computation Conference (PSCC’05), (2005), 1–7.

[8]. Altaie A.S., “Design of a New Digital Relay for Transmission Line Fault Detection, Classification and Localization Based on a New Composite Relay and Artificial Neural Network Approach,” Western Michigan University, (2015).

[9]. Ngo Minh Khoa D.T.V., Nguyen Huu Hieu2, “A Study of SVC’s Impact Simulation and Analysis for Distance Protection Relay on Transmission Lines,” Int. J. Electr. Comput. Eng., (2017), 7, 4, 1686–1695.

[10]. Sybille P.G., “SVC (Detailed Model).” [Online]. Available: https://www.mathworks.com/help/physmod/sps/examples/svc-detailed-model.html. [Accessed: 08-Jul-2019].

[11]. Al-Husban A.N., “An Eigenstructure Assignment for a Static Synchronous Compensator,” Am. J. Eng. Appl. Sci., (2009), 2, 4, 812–816.

[12]. Le Ngoc Giang T.T.N., Nguyen Thi Dieu Thuy, “Assessment study of STATCOM’s effectiveness in improving transient stability for power system,” TELKOMNIKA, (2013), 11, 10, 6095–6104.